Enhancing Polo-like Kinase 1 Selectivity of Polo-box Domain-binding Peptides

Xue Zhi Zhao, **David Hymel**, and **Terrence R. Burke Jr.**[*]

Chemical Biology Laboratory, Center for Cancer Research, National Cancer Institute, National Institutes of Health, Frederick, Maryland 21702

Abstract

An important goal in the development of polo-like kinase 1 (Plk1) polo-box domain (PBD) binding inhibitors is selectivity for Plk1 relative to Plk2 and Plk3. In our current work we show that Plk1 PBD selectivity can be significantly enhanced by modulating interactions within a previously discovered "cryptic pocket" and a more recently identified proximal "auxiliary pocket."

Graphical Abstract
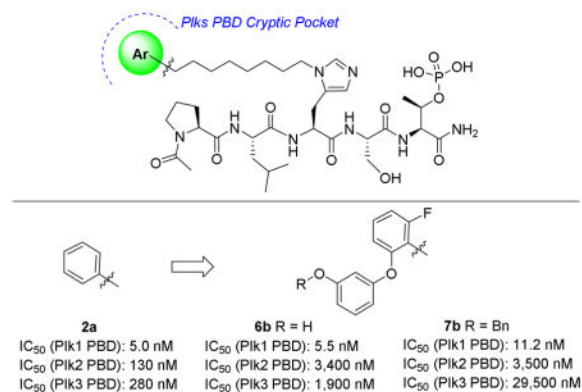
Keywords

Plk1; Selectivity; Polo-box domain; Cryptic binding pocket

[*]Corresponding Author: Tel: 301-846-5906, Fax: 301-846-6033, burkete@helix.nih.gov.

1. Introduction

Members of the polo family of serine/threonine kinases (polo-like kinases; Plks 1–5) play important roles in mammalian cellular physiology.[1] Overexpression of the cell cycle regulatory Plk1 occurs in a number of cancers, where it is associated with a poor prognosis and Plk1 is recognized as a potentially promising anti-cancer target.[2] In addition to their amino-terminal catalytic kinase domains (KD) (not present in Plk5[3]), the Plks are characterized by C-terminal polo-box domains (PBDs), which mediate protein-protein interactions (PPIs) by recognizing and binding to phosphoserine (pSer) and phosphothreonine (pThr)-containing sequences.[4] Development of Plk1 inhibitors is made complicated by a number of factors. Among these is the fact that Plks 2 and 3 may function as tumor suppressors, thereby making Plk1-selectivity an important objective.[5] Issues of collateral cytotoxicity have arisen for KD-directed inhibitors, potentially due to similarities among the KDs of Plk1, 2 and 3 as well as high homology among protein kinases in general. Because both the KD and PBD are essential for proper Plk function,[6] PBD-binding antagonists offer a potentially attractive alternative to KD-directed inhibitors for down-regulating Plk function.[7] Such agents may offer advantages in terms of selectivity, since PBDs are unique to the Plks and the domains exhibit differences in their binding preferences for phosphoepitope sequences.[8,9] Additionally, the results of blocking PBD-binding may not be the same as inhibiting kinase activity, opening the possibility of qualitatively different therapeutic profiles or synergism with KD inhibitors.[10] Accordingly, significant effort has been devoted to develop Plk1 PBD-binding antagonists.[2,7]

Competitive PBD-binding inhibitors have been approached using peptides or peptide mimetics, which are based on cognate recognition sequences. Starting from the polo-box interacting protein 1 (PBIP) pT78-derived peptide PLHSpT (**1**),[11] we have previously reported that appending alkylphenyl groups from different positions on the peptide, including the His N(π)-position [the sequence having a $(CH_2)_8Ph$ group appended is designated as PLH*SpT (**2a**)],[12] the 4-position on the Pro residue (**3**)[13] and an amino-terminal *N*-alkyl Gly residue (**4**),[14] can result in up to one thousand-fold enhancement in Plk1 PBD-binding affinity (Figure 1). We found in each case that the alkylphenyl groups bind within a "cryptic binding pocket" on the PBD surface, which is defined by PBD residues Y417, Y421, Y481, L478, F482 and Y485 and revealed by rotation of the Y481 side chain (Figure 2). Abell has also shown that the same cryptic pocket can be accessed by the phenyl ring of the terminal Phe residue in the longer PBIP1 pT78-derived sequence FDPPLHSpTA[15] and by the phenyl ring of 3-phenylpropylamide on the Pro residue of **1**.[16] This group has also shown that higher affinity can be realized by replacing the terminal Phe residue in the FDPPLHSpTA sequence with a residue that contains a more lipophilic 2-benzothiophene ring (**5**), which is consistent with the highly lipophilic nature of the cryptic pocket (Figure 1).[17]

Recently, we examined access to the cryptic pocket from the His N(π)-position in peptide **1** using an oxime-based post-solid phase peptide diversification strategy[18] and found that replacing the phenyl ring with motifs having two aryl rings arranged in an angular orientation, can result in several fold greater Plk1 PBD-binding affinity relative to the parent phenyl ring.[19] We hypothesized that enhanced affinity may result from interactions within an

auxiliary region that is contiguous with the canonical cryptic pocket. Yet, beyond the above, very little has been reported to exploit binding within the cryptic pocket to greater advantage. Therefore, as we report herein, we used the simple tethered phenyl ring of peptide **2a** and our recently disclosed 2-fluoro-6-phenyloxylphenyl peptide **2b** as starting points for the design of peptides **6a** and **6b**, which include hydroxyls at different locations. Our thought was that this added functionality could potentially afford interactions with hydroxyl or carbonyl groups of residues Y421 and Y481 or other residues proximal to the Plk1 PBD cryptic pocket. The benzyl protected precursors **7a** and **7b** also provided the opportunity to extend aromatic interactions in this region. Our ultimate goal was to more fully explore what could be achieved by altering known binding motifs, particularly effects related to Plk1, 2 and 3 selectivity.

2. Results and discussion

2.1. Chemistry

Peptides **6(a, b)** and **7(a, b)** were obtained by Fmoc-based solid-phase peptide synthesis using reagents **18(a-d)**, which were prepared as shown in Scheme 1.[20] The synthesis began with the *t*-butyl and benzyl-protected alcohols **9(a, b)**, which were synthesized by protecting the free hydroxyl of the commercially available alcohol 2-(4-bomophenyl)ethan-1-ol (**8**). Coupling of the aryl bromides **9(a, b)** and oct-7-yn-1-ol,[21] followed by hydrogenation catalyzed by Pd·C (for **10a**) or Wilkinson's catalyst (for **10b**) afforded alcohols **11(a, b)** having *t*-butyl and benzyl protecting groups, respectively. Separately, SNAr reaction of 2,6-difluorbenzaldehyde (**12**) with 3-(*tert*-butoxy)phenol or 3-(benzyloxy)phenol gave the 2-fluoro-6-phenoxybenzaldehydes **13(a, b)**, respectively.[22] Reduction of the aldehyde functionality in **13(a, b)** and replacement of the hydroxyls in the resulting **14(a, b)** with bromide gave the corresponding benzyl bromides **15(a, b)**. Coupling of **15(a, b)** with hept-6-yn-1-ol or ((hept-6-yn-1-yloxy)methyl)benzene afforded the alkynes **16(a, b)**. Hydrogenation catalyzed by Pd·C or Wilkinson's catalyst afforded the alcohols **17(a, b)**. Finally, reaction of alcohols **11(a, b)** and **17(a, b)** with either the 2,4-dimethoxylbenzyl ester or the benzyl ester of N^α-Fmoc-His using our previously reported methodology afforded the key orthogonally protected His N(π)-alkylated analogs **18(a-d)**.[19,20] Employing these reagents, we prepared peptides **19(a-d)** on NovaSyn TGR resin. Cleavage of the peptides from the resin using a cocktail solution of TFA/H_2O/TIS (95/2.5/2.5) and purification by HPLC gave the desired peptide products **6(a, b)** and **7(a, b)** (Scheme 1).

2.3. Biological evaluation

2.3.1. PBD-binding activity in full-length Plk1—In order to evaluate PBD-binding affinities, we employed an ELISA assay, which measures the ability of the synthetic peptides to compete with an immobilized phosphopeptide "PMQSpTPLN" for binding to full-length Plk1.[19] As we have recently reported, the parent peptide **1**, which lacks an N(π)-alkyl group, shows almost no inhibitory potency in this assay ($IC_{50} > 300$ μM), while introduction of a -[CH_2]$_8$Ph at this position results in greater than an approximate 1000-fold enhancement in binding affinity (**2a**, $IC_{50} = 180$ nM, Table 1).[19] Replacement of the phenyl ring in **2a** with a 2-fluoro-6-phenoxybenzy group resulted in enhanced binding affinity (**2b**, $IC_{50} = 127$ nM).[19] The focus of our current study was to examine the effects of introducing additional

oxygen functionality into cryptic pocket-binding motifs. For this purpose, we prepared **6a** as a 4-(2-hydroxyethyl)-containing analog of **2a** and **6b** as an analog of **2b**, which included a 3-hydroxyl group at the 3-position of the phenyl ether moiety. Both **6a** and **6b** exhibited IC_{50} values (220 nM and 190 nM, respectively), which were approximately equal to **2a**, indicating that the presence of the hydroxyl groups was compatible with maintenance of high affinity binding (Table 1). Given the large number of aromatic side chains bordering the cryptic pocket, we were also interested in observing the effects incurred by introducing additional aryl functionality. Peptides **7a** and **7b**, which are intermediates in the synthesis of **6a** and **6b**, respectively served this purpose. While the added benzyl group was well tolerated in **7a** (IC_{50} = 150 nM), its presence in **7b** caused an approximate four-fold loss of potency (IC_{50} = 860 nM) (Table 1).

2.3.2. Binding affinities measured using isolated PBDs of Plk1, 2 and 3—An

important consideration in the development of PBD-binding inhibitors is selectivity for the PBD of Plk1 relative the PBDs of Plk2 and Plk3. While, there are no PBD-binding assays currently available that employ full-length Plk2 and Plk3, fluorescence polarization (FP) assays have been reported, which measure the abilities of inhibitors to compete with fluorescently labeled pThr-containing peptides for binding to the isolated PBDs of Plk1, 2 and 3.[8,9] These assays employ fluorescently labeled peptides that have been optimized for binding to each individual PBD isoform.[8,9] It is worth noting that the IC_{50} values measured against the isolated Plk1 PBD are more potent than those measured against full length Plk1.[23,24] This difference can be attributed to inhibitory interactions between the PBD and KD, which affect equilibrium binding to phosphopeptides. We measured the abilities of **6(a, b)** and **7(a, b)** as well as **2(a, b)** to compete with fluorescently-labeled phosphopeptide probes for binding to isolated PBDs of Plks 1–3 using FP assays (Table 1).

While the parent peptide **2a** showed approximately 20-fold selectivity for the Plk1 PBD relative to the Plk2 and approximately 50-fold selectivity relative to the Plk3 PBD, introduction of functionality onto the cryptic pocket-binding phenyl ring of **2a** was capable of further increasing selectivity for both domains (Table 1). Fold-selectivities for Plk1 relative to Plk2 and Plk3, respectively upon introduction of the indicated functionality were: 4-(2-hydroxylethyl) (**6a**) 50 and 175; 2-fluoro, 6-phenlyoxy (**2b**) 40 and 200; 2-fluoro, 6-(3-hydroxy)phenyloxy (**6b**) 60 and 350. Interestingly, introducing a benzyl group onto **6b** to give 2-fluoro, 6-(3-benzyloxy)phenoxy-containing **7b**, increased Plk1 PBD selectivity versus the Plk2 PBD to 300-fold and 2,500-fold relative to the Plk3 PBD. This data showed that modification of the phenyl group in **2a** could result in significant improvements in selectivity for the Plk1 PBD relative to the Plk2 PBD and that near complete selectivity over the Plk3 PBD could be realized.

2.4 Comparison of the cryptic pocket of the Plk1 PBD with potential cryptic pockets in the PBDs of Plk2 and Plk3

A major focus of our current study was to examine the effects incurred by modifying interactions within the cryptic binding pocket. Although we prepared only a very limited number of analogs, we found that changes to the cryptic pocket-binding phenyl ring could have a profound impact on the selectivity for the Plk1 PBD relative to the Plk2 and Plk3

PBDs. We speculated whether there might be differences among the PBDs of Plk1, 2 and 3, which could potentially contribute to modulation of selectivity. The existence of "cryptic binding pockets" in the Plk2 and Plk3 PBDs have not been reported. Crystal structures of the Plk2 PBD are known,[25,26] yet these structures do not contain bound ligands and to date, no crystal structures of the Plk3 PBD have been reported. Therefore, we set out to define putative interacting residues within potential cryptic pockets of Plk2 and Plk3 and to compare them with corresponding residues in the Plk1 PBD.

Lacking a crystal structure for the Plk3 PBD, we aligned the sequences of Plk1 with Plk3 and identified residues of Plk3 that corresponded to the Plk1 PBD. We then generated a homology model of the Plk3 PBD based on the Plk1 PBD (PDB accession code: 3FVH) through the online Robetta server.[27] Using the crystal structure of the Plk1 PBD having ligand **2a** bound (PDB accession code: 3RQ7) we superimposed the crystal structure of the apo Plk2 PBD (PDB accession code: 4RS6) and the Plk3 PBD homology model. Ligand **2a** was oriented into the Plk2 and Plk3 PBDs as in the Plk1 PBD and residues proximal to the ligands were minimized (Figure 3). We found that all three PBDs were highly similar in the region of the cryptic pocket. Several of the residues from Plk1 (creme; Y417, Y421, Y481, F482 and Y485) and Plk2 (orange; Y510, Y514, Y574, F575 and Y578) are closely oriented. Although these residues were also found in the Plk3 PBD, certain side chains were rotated or slightly displaced in the latter domain (blue; Y470, F474, Y534, F535 and Y538) (Figure 3). Notable differences among the tree domains appeared to be a single residue at the terminus of the pocket, which consisted of L478, V571 and I531 for Plk1, Plk2 and Plk3, respectively. Additionally, while similar orientations were observed for K513 and K473 in Plk2 and Plk3, respectively, the corresponding K420 in Plk1 was considerably displaced. The most significant variations were in residues bordering a recently identified "auxiliary binding region", which is contiguous with the canonical cryptic pocket.[19] Here the differences for Plk1, Plk2 and Plk3 were found to be N484, H577 and S537; E488, E581 and Q541 and H489, N582 and H542, respectively. In spite of the general overall high similarity of residues proximal to the cryptic pocket among the three PBDs, it is possible that the minor differences noted as well as the significant variations in the auxiliary pocket could potentially contribute to significant modulation of ligand recognition. Although beyond the scope of the current work, replacing select residues identified above in the PBDs of Plk2 and Plk3 could help to resolve speculation regarding the roles that these may play in ligand selectivity.

3. Conclusions

Targeting the PBD offers a conceptually attractive alternative to KD-directed inhibitors for down-regulating Plk1 function.[2,7] Achieving selectivity is an important consideration in the development of Plk1 PBD-binding inhibitors. In our current work we demonstrate that structural variation of functionality intended to interact within the cryptic pocket can have a significant impact on the relative affinities of peptides for the PBDs of Plk2 and Plk3 relative to Plk1. In the case of Plk3, specificity can exceed three orders-of-magnitude. We have found subtle differences in residues proximal to the putative cryptic pockets and particularly in residues forming a recently identified proximal auxiliary binding pocket. We suggest that these differences may contribute to ligand selectivity. Introducing extended functionality that

permits access to the auxiliary pocket may be a valuable approach to increasing differences in binding affinity among the three domains.

A further significant challenge in developing clinically relevant PBD-binding inhibitors arises from the fact that PBD-binding peptides and peptide mimetics, even those showing extremely high affinities in extracellular assays, have frequently shown disappointing biological efficacies in cell-based systems.[12] The discrepancies in potencies may result from poor cellular uptake. Accordingly, increasing cellular bioavailability of PBD-binding inhibitors represents an active area of investigation.[28] Our current peptides are not clinically relevant, due in part to poor bioavailability. However, given the extreme enhancement in overall ligand affinity that can be achieved by accessing the cryptic pocket, we believe that optimizing interactions within this region may be highly relevant to developing more bioavailable agents. Accordingly, our current findings may facilitate the further development of clinical agents.

4. Experimental Section

4.1. General chemical methods

Proton (^{1}H) and carbon (^{13}C) NMR spectra were recorded on a Varian 400 MHz spectrometer or a Varian 500 MHz spectrometer and are reported in ppm relative to TMS and referenced to the solvent in which the spectra were collected. Solvent was removed by rotary evaporation under reduced pressure and anhydrous solvents were obtained commercially and used without further drying. Purification by silica gel chromatography was performed using Combiflash with EtOAc–hexanes or CH_2Cl_2-MeOH solvent systems. Electrospray ionization-mass spectrometra (ESI-MS) were acquired with an Agilent LC/MSD system equipped with a multimode ion source. High resolution mass spectrometric (HRMS) were acquired with a LTQ-Orbitrap-XL at 30 K resolution by LC/MS-ESI.

4.1.1. General procedure A for the synthesis of alkynes (10a, b) using Sonogashira reaction[21]—Appropriate terminal alkynes (0.45 mmol) were added to a mixture of bromides (**9a**, **b**) (0.3 mmol) and bis(triphenylphosphine)palladium (II) dichloride (9 μmol), DIEA (0.3 mmol) and copper (I) iodide (0.03 mmol) in DMF (1.5 mL). The reaction mixture was sealed and heated under argon (70 °C, 18 h). The crude mixture was purified by silica gel chromatography to provide alkynes (**10a**, **b**).

4.1.2. General procedure B for the synthesis of alcohols (11a, 17a) using Wilkinson's catalyst[29]—A mixture of alkynes (**10a**, **16a**) (1.0 mmol), tris(triphenylphosphine)rhodium(I) chloride (0.1 mmol) in THF (10 mL) and ^{t}BuOH (10 mL) was stirred under H_2 (16 h). The crude mixture was purified by silica gel chromatography to provide alcohols (**11a**, **17a**).

4.1.3. General procedure C for the synthesis of alcohols (11b, 17b) using Pd·C—To a solution of alkynes (**10b**, **16b**) (10 mmol) in MeOH (10 mL) was added Pd·C (30 mg, 10%) and the mixture was hydrogenated under H_2. When all starting material had been consumed (TLC), the reaction mixture was collected by filtration and concentrated. The crude residue was purified by silica gel chromatography to provide alcohols (**11b**, **17b**).

4.1.4. General procedure D for the synthesis of aldehydes (13a, b)[22]—Potassium carbonate (100 mmol) was added to a solution of 2,6-difluorobenzaldehydes (**12a**) (102 mmol) and 3-(benzyloxy)phenol or 3-(*tert*-butoxy) phenol (100 mmol) in dimethylacetamide (DMA) (50 mL). The reaction mixture was stirred and refluxed (2 h). The crude mixture was partitioned between CH_2Cl_2 and H_2O, dried (Na_2SO_4), concentrated and purified by silica gel chromatography to provide aldehydes (**13a**, **b**).

4.1.5. General procedure E for the synthesis of benzylalcohols (14a, b)—$NaBH_4$ (20 mmol) was added portion-wise to the solution of aldehydes (**13a**, **b**) (20 mmol) in MeOH (100 mL) (0 °C). The reaction mixture was stirred (0 °C, 0.5 h) and concentrated. The crude mixture was partitioned between EtOAc and H_2O, dried (Na_2SO_4), concentrated and purified by silica gel chromatography to provide benzylalcohols (**14a**, **b**).

4.1.6. General procedure F for the synthesis of benzylbromide (15a, b)—PPh_3 (30 mmol) was added to a solution of benzylalcohols (**14a**, **b**) (20 mmol) in acetonitrile (100 mL). CBr_4 (30 mmol) was added (0 °C). The formed suspension was stirred (30 min). The mixture was filtered and the filtrate was concentrated. The crude residue was purified by silica gel chromatography to provide benzylbromides (**15a**, **b**).

4.1.7. General procedure G for the synthesis of N^π-alkylated His residues (18a–d)[19,20]—According to our previous reports,[19,20] a solution of alcohols (**11a**, **b** and **17a**, **b**) (2 mmol) and DIEA (2 mmol) in CH_2Cl_2 (1.5 mL) was added dropwise to a solution of trifluoromethanesulfonic anhydride (2 mmol, 1.0 M in CH_2Cl_2) in CH_2Cl_2 (2.5 mL) under argon (−78° C) and stirred (20 min). A solution of 2,4-dimethoxybenzyl N^α-Fmoc-N^τ-Trt-*L*-histidinate (2 mmol) or benzyl N^α-Fmoc-N^τ-Trt-*L*-histidinate (2 mmol) in CH_2Cl_2 (5 mL) was added (−78 °C). The mixture was stirred (16 h) and concentrated. The residue was deprotected using TFA:TIS (10:1, 10 mL) or hydrogenated using Pd·C (10%) in MeOH. The resultant crude residue was purified by silica gel chromatography to provide N^π-alkylated His residues (**18a–d**).

4.1.8. 1-Bromo-4-(2-(*tert*-butoxy)ethyl)benzene (9a).[30]—Magnesium perchlorate (0.96 g, 4.3 mmol) and commercial available 2-(4-bromophenyl)ethanol **8** (8.6 g, 43 mmol) were dissolved in DCM (50 mL). (Boc)$_2$O (21 g, 98 mmol) was added to the suspension. The mixture was stirred (35 °C, 16 h) and concentrated. The crude residue was purified by silica gel column chromatography to provide **9a** as a colorless oil (7.6 g, 69% yield). ^{1}H NMR (400 MHz, CDCl$_3$) δ 7.42 (d, J = 8.3 Hz, 2H), 7.13 (d, J = 8.3 Hz, 2H), 3.54 (t, J = 7.2 Hz, 2H), 2.79 (t, J = 7.1 Hz, 2H), 1.18 (s, 9H). ^{13}C NMR (100 MHz, CDCl$_3$) δ 138.57, 131.22 (2C), 130.79 (2C), 119.85, 72.90, 62.56, 36.78, 27.50 (3C).

4.1.9. 1-(2-(Benzyloxy)ethyl)-4-bromobenzene (9b)—2-(4-Bromophenyl)ethanol **8** (3.2 g, 16 mmol) and (bromomethyl)benzene (1.9 mL, 16 mmol) were dissolved in THF (50 mL). NaH (0.45 g, 18 mmol) was added (0 °C). The reaction mixture was stirred (from 0 °C to room temperature, 16 h), quenched by pouring into water, extracted by EtOAc, dried (Na_2SO_4) and concentrated. The crude residue was purified by silica gel chromatography to provide **9b** as a colorless oil (1.9 g, 41% yield). ^{1}H NMR (400 MHz, CDCl$_3$) δ 7.45 - 7.43

(m, 2H), 7.39 - 7.31 (m, 5H), 7.15 - 7.13 (m, 2H), 4.55 (s, 2H), 3.70 (t, J = 6.9 Hz, 2H), 2.91 (t, J = 6.9 Hz, 2H).^{13}C NMR (101 MHz, CDCl$_3$) δ 138.26, 138.13, 131.38 (2C), 130.72 (2C), 128.40 (2C), 127.61 (3C), 120.03, 73.03, 70.77, 35.80.

4.1.10. 8-(4-(2-(*tert*-Butoxy)ethyl)phenyl)oct-7-yn-1-ol (10a)—Treatment of **9a** and commercial available oct-7-yn-1-ol as outlined in general procedure A provided **10a** as a yellow oil (41% yield). ^{1}H NMR (400 MHz, CDCl$_3$) δ 7.32 (d, J = 8.1 Hz, 2H), 7.15 (d, J = 8.1 Hz, 2H), 3.66 (td, J = 6.6, 5.3 Hz, 2H), 3.53 (t, J = 7.3 Hz, 2H), 2.81 (t, J = 7.3 Hz, 2H), 2.42 (t, J = 7.0 Hz, 2H), 1.66 - 1.58 (m, 5H), 1.54 - 1.48 (m, 2H), 1.47 - 1.40 (m, 2H), 1.17 (s, 9H). ^{13}C NMR (101 MHz, CDCl$_3$) δ 139.02, 131.36 (2C), 128.90 (2C), 121.67, 89.66, 80.67, 72.92, 62.86, 62.72, 37.24, 32.66, 28.73, 28.68, 27.49 (3C), 25.32, 19.36. ESI-MS *m/z*: 325.2 (MNa$^+$).

4.1.11. 8-(4-(2-(Benzyloxy)ethyl)phenyl)oct-7-yn-1-ol (10b)—Treatment of **9b** with commercial available oct-7-yn-1-ol as outlined in general procedure A provided **10b** as a yellow oil (62% yield). ^{1}H NMR (400 MHz, CDCl$_3$) δ 7.37 - 7.29 (m, 7H), 7.16 (d, J = 8.1 Hz, 2H), 4.53 (s, 2H), 3.68 (dt, J = 9.2, 6.8 Hz, 4H), 2.94 - 2.91 (m, 2H), 2.43 (t, J = 7.0 Hz, 2H), 1.74 (bs, 1H), 1.68 - 1.60 (m, 4H), 1.55 - 1.48 (m, 2H), 1.47 - 1.41 (m, 2H).

4.1.12. 8-(4-(2-(*tert*-Butoxy)ethyl)phenyl)octan-1-ol (11a)—Treatment of **10a** as outlined in general procedure C provided **11a** as a yellow solid (54% yield). ^{1}H NMR (400 MHz, CDCl$_3$) δ 7.17 - 7.11 (m, 4H), 3.65 (t, J = 6.6 Hz, 2H), 3.55 (t, J = 7.7 Hz, 2H), 2.82 (t, J = 7.7 Hz, 2H), 2.59 (t, J = 7.7 Hz, 2H), 11.63 - 1.56 (m, 4H), 1.40 - 1.30 (m, 8H), 1.21 (s, 9H). ^{13}C NMR (101 MHz, CDCl$_3$) δ 140.60, 136.39, 128.85 (2C), 128.27 (2C), 72.90, 63.25, 63.03, 37.08, 35.56, 32.78, 31.53, 29.47, 29.36, 29.25, 27.55 (3C), 25.74. APCI-MS *m/z*: 307.2 (MNa$^+$).

4.1.13. 8-(4-(2-(Benzyloxy)ethyl)phenyl)octan-1-ol (11b)—Treatment of **10b** as outlined in general procedure B provided **11b** as a colorless oil (29% yield). ^{1}H NMR (400 MHz, CDCl$_3$) δ 7.39 - 7.29 (m, 5H), 7.23 - 7.22 (m, 1H), 7.18 - 7.12 (m, 3H), 4.56 (s, 2H), 3.72 (q, J = 7.1 Hz, 2H), 3.65 (td, J = 6.6, 4.5 Hz, 2H), 2.94 (t, J = 7.2 Hz, 2H), 2.62 - 2.58 (m, 1H), 1.65 - 1.50 (m, 6H), 1.40 - 1.30 (m, 7H). ^{13}C NMR (101 MHz, CDCl$_3$) δ 140.72, 138.45, 136.04, 128.80 (2C), 128.38 (2C), 128.36 (2C), 127.64 (2C), 127.53 (2C), 72.95, 71.41, 63.05, 35.96, 35.57, 32.79, 31.54, 29.48, 29.37, 29.26, 25.75. DUIS-MS *m/z*: 341 (MH$^+$).

4.1.14. 2-(3-(*tert*-Butoxy)phenoxy)-6-fluorobenzaldehyde (13a)—Treatment of commercial available 2,6-difluorobenzaldehyde **12** and 3-(*tert*-butoxy)phenol as outlined in general procedure D provided **13a** as a yellow oil (78% yield). ^{1}H NMR (400 MHz, CDCl$_3$) δ 10.51 (s, 1H), 7.46 - 7.40 (m, 1H), 7.31 - 7.27 (m, 1H), 6.89 - 6.80 (m, 3H),6.73 (t, J = 2.2 Hz, 1H), 6.66 (d, J = 8.4 Hz, 1H), 1.37 (s, 9H).^{13}C NMR (101 MHz, CDCl$_3$) δ 186.78 (d, J = 2.4 Hz), 162.90 (d, J = 263.4 Hz), 160.43 (d, J = 5.2 Hz), 157.14, 155.93, 135.69 (d, J = 11.6 Hz), 129.90, 120.42, 115.95 (d, J = 9.4 Hz), 115.65, 114.64, 113.41 (d, J = 3.8 Hz), 110.77 (d, J = 21.2 Hz), 79.24, 28.84 (3C). ESI-MS *m/z*: 271.1 (MH$^+$-OH), 311.1 (MNa$^+$). [3-(*tert*-butoxy) phenol was prepared from commercial available 3-(benzyloxy)phenol

through two steps below.[30] Magnesium perchlorate (0.56 g, 2.5 mmol) and 3-(benzyloxy)phenol (5 g, 25 mmol) were dissolved in DCM (50 mL). (Boc)$_2$O (12.5 g, 57 mmol) was added. The formed brown solution was stirred (35 °C, 16h) and concentrated. The crude residue was purified by silica gel chromatography to provide 1-(benzyloxy)-3-(*tert*-butoxy)benzene as a colorless oil (4.6 g, 72% yield). ^{1}H NMR (400 MHz, CDCl$_3$) δ 7.49 - 7.34 (m, 5H), 7.21 (t, J = 8.2 Hz, 1H), 6.77 (dd, J = 7.9, 1.9 Hz, 1H), 6.69 - 6.66 (m, 2H), 5.08 (s, 2H), 1.39 (s, 9H). ^{13}C NMR (100 MHz, CDCl$_3$) δ 159.36, 156.62, 137.06, 129.15, 128.59 (2C), 127.96, 127.54 (2C), 116.73, 111.10, 109.87, 78.64, 70.08, 28.93 (2C). Hydrogenation of 1-(benzyloxy)-3-(*tert*-butoxy) benzene (4.0 g, 15.9 mmol) using Pd·C (10%, 60 mg) in MeOH (50 mL) (4 h) provided 3-(*tert*-butoxy)phenol a yellow solid (2.4 g, 93% yield). ^{1}H NMR (400 MHz, CDCl$_3$) δ 7.10 (t, J = 8.1 Hz, 1H), 7.05 (brs, 1H), 6.61 (ddd, J = 8.1, 2.4, 1.5 Hz, 2H), 6.55 (t, J = 2.3 Hz, 1H), 1.35 (s, 9H). ^{13}C NMR (101 MHz, CDCl$_3$) δ 156.37, 155.67, 129.51, 116.52, 111.83, 111.31, 79.73, 28.79 (3C). ESI-MS m/z: 167.1 (MH$^+$).]

4.1.15. 2-(3-(Benzyloxy)phenoxy)-6-fluorobenzaldehyde (13b)—Treatment of commercial available 2,6-difluorobenzaldehyde (**12**) with 3-(benzyloxy)phenol as outlined in general procedure D provided **13b** as a brown oil (18% yield). ^{1}H NMR (400 MHz, CDCl$_3$) δ 10.40 (s, 1H), 7.37 - 7.18 (m, 7H), 6.82 - 6.77 (m, 1H), 6.75 (dd, J = 8.3, 2.3 Hz, 1H), 6.61 - 6.58 (m, 3H), 4.97 (s, 2H). ^{13}C NMR (101 MHz, CDCl$_3$) δ 186.76, 162.90 (d, J = 263.5 Hz), 160.28, 160.08 (d, J = 5.2 Hz), 156.88, 136.42, 135.69 (d, J = 11.6 Hz), 130.61, 128.65 (2C), 128.14, 127.51 (2C), 116.21 (d, J = 9.5 Hz), 113.97 (d, J = 3.7 Hz), 111.97, 111.25, 111.05 (d, J = 21.2 Hz), 106.67, 70.26.

4.1.16. (2-(3-(*tert*-Butoxy)phenoxy)-6-fluorophenyl)methanol (14a)—Treatment of **13a** as outlined in general procedure E provided **14a** as a colorless oil (93% yield). ^{1}H NMR (400 MHz, CDCl$_3$) δ 7.24 (t, J = 8.1 Hz, 1H), 7.21 - 7.17 (m, 1H), 6.87 - 6.80 (m, 2H), 6.77 - 6.74 (m, 1H), 6.69 (t, J = 2.3 Hz, 1H), 6.65 (d, J = 8.5 Hz, 1H), 4.83 (d, J = 1.0 Hz, 2H), 2.32 (brs, 1H), 1.36 (s, 9H). ^{13}C NMR (101 MHz, CDCl$_3$) δ 161.68 (d, J = 247.3 Hz), 156.97 (2C), 156.91 (d, J = 7.4 Hz), 129.67, 129.53 (d, J = 10.4 Hz), 119.59, 119.34 (d, J = 18.1 Hz), 114.93, 113.89, 113.71 (d, J = 3.3 Hz), 110.44 (d, J = 22.6 Hz), 79.06, 53.97 (d, J = 4.9 Hz), 28.84 (3C). ESI-MS m/z: 291.1 (MH$^+$), 313.1 (MNa$^+$).

4.1.17. (2-(3-(Benzyloxy)phenoxy)-6-fluorophenyl)methanol (14b)—Treatment of **13b** as outlined in general procedure E provided **14b** as a colorless oil (79% yield). ^{1}H NMR (400 MHz, CDCl$_3$) δ 7.46 - 7.34 (m, 5H), 7.30 - 7.26 (m, 1H), 7.25 - 7.20 (m, 1H), 6.92 - 6.87 (m, 1H), 6.80 (ddd, J = 8.4, 2.4, 0.9 Hz, 1H), 6.72 - 6.63 (m, 3H), 5.06 (s, 2H), 4.83 (d, J = 1.4 Hz, 2H), 2.18 (S, 1H). ^{13}C NMR (101 MHz, CDCl$_3$) δ 161.71 (d, J = 247.6 Hz), 160.20, 157.94, 156.52 (d, J = 7.3 Hz), 136.57, 130.44, 129.63 (d, J = 10.4 Hz), 128.64 (2C), 128.11, 127.54 (2C), 119.67 (d, J = 17.9 Hz), 114.34 (d, J = 3.3 Hz), 111.18, 110.75 (d, J = 22.5 Hz), 110.41, 105.81, 70.20, 54.04 (d, J = 5.1 Hz).

4.1.18. 2-(Bromomethyl)-1-(3-(*tert*-butoxy)phenoxy)-3-fluorobenzene (15a)—
Treatment of **14a** as outlined in general procedure F provided **15a** as a colorless oil (90% yield). ^{1}H NMR (400 MHz, CDCl$_3$) δ 7.29 - 7.25 (m, 1H), 7.21 (td, J = 8.4, 6.5 Hz, 1H),

6.86 - 6.80 (m, 3H), 6.73 (t, J = 2.3 Hz, 1H), 6.63 (d, J = 8.5 Hz, 1H), 4.67 (s, 2H), 1.38 (s, 9H). ^{13}C NMR (101 MHz, CDCl$_3$) δ 161.51 (d, J = 250.4 Hz), 156.95, 156.82 (d, J = 6.5 Hz), 156.73, 130.11 (d, J = 10.6 Hz), 129.65, 119.87, 117.08 (d, J = 17.2 Hz), 115.38, 114.44, 113.50 (d, J = 3.3 Hz), 110.11 (d, J = 21.6 Hz), 79.07, 28.87 (3C), 20.03 (d, J = 5.4 Hz).

4.1.19. 1-(3-(Benzyloxy)phenoxy)-2-(bromomethyl)-3-fluorobenzene (15b)—

Treatment of **14b** as outlined in general procedure F provided **15b** as a colorless oil (87% yield). ^{1}H NMR (400 MHz, CDCl$_3$) δ 7.33 - 7.23 (m, 5H), 7.19 - 7.14 (m, 1H), 7.12 - 7.06 (m, 1H), 6.76 - 6.68 (m, 2H), 6.60 - 6.52 (m, 3H), 4.94 (s, 2H), 4.53 (d, J = 1.4 Hz, 2H). ^{13}C NMR (101 MHz, CDCl$_3$) δ 161.54 (d, J = 250.6 Hz), 160.18, 157.57, 156.51 (d, J = 6.5 Hz), 136.59, 130.40, 130.18 (d, J = 10.4 Hz), 128.65 (2C), 128.11, 127.57 (2C), 117.34 (d, J = 17.1 Hz), 113.93 (d, J = 3.3 Hz), 111.80, 110.74, 110.35 (d, J = 21.6 Hz), 106.37, 70.21, 20.04 (d, J = 5.4 Hz). APCI-MS m/z: 387.0, 389.0 (MH$^+$).

4.1.20. 2-(8-(Benzyloxy)oct-2-yn-1-yl)-1-(3-(*tert*-butoxy)phenoxy)-3-fluorobenzene (16a).[31]—

A solution of butyllithium in hexanes (10 mmol, 2.5 M) was added dropwise to a solution of ((hept-6-yn-1-yloxy)methyl)benzene (10 mmol) [which was prepared from commercial available hept-6-yn-1-ol using BnBr and NaH in THF (0°C) (78% yield). 1H NMR (400 MHz, CDCl3) δ 7.37 - 7.35 (m, 4H), 7.33 - 7.29 (m, 1H), 4.53 (s, 2H), 3.50 (t, J = 6.5 Hz, 2H), 2.22 (td, J = 6.8, 2.6 Hz, 2H), 1.96 (t, J = 2.6 Hz, 1H), 1.71 - 1.61 (m, 2H), 1.60 - 1.47 (m, 4H). 13C NMR (101 MHz, CDCl3) δ 138.65, 128.36 (2C), 127.62, 127.50 (2C), 84.53, 72.92, 70.23, 68.29, 29.29, 28.34, 25.42, 18.39. ESI-MS m/z: 203.1 (MH+).] in THF (20 mL) (−78 °C). The mixture was stirred (−78 °C, 1 h). The solution of benzylbromides (**15a**) (3 mmol) in THF (10 mL) was added. The reaction mixture was stirred (−78 °C to room temperature, 16 h), quenched by pouring into ice, extracted by EtOAc and concentrated. The crude residue was purified by silica gel chromatography to provide benzylalkynes (**16a**) as a colorless oil (77% yield). ^{1}H NMR (400 MHz, CDCl$_3$) δ 7.38 - 7.3 (m, 4H), 7.33 - 7.27 (m, 1H), 7.21 (t, J = 8.2 Hz, 1H), 7.15 (td, J = 8.3, 6.5 Hz, 1H), 6.85 (t, J = 8.7 Hz, 1H), 6.79 - 6.72 (m, 2H), 6.67 (dd, J = 5.3, 3.0 Hz, 2H), 4.51 (s, 2H), 3.59 (brs, 2H), 3.46 (t, J = 6.6 Hz, 2H), 2.11 - 2.07 (m, 2H), 1.64 - 1.57 (m, 2H), 1.47 - 1.39 (m, 4H), 1.36 (s, 9H). ^{13}C NMR (101 MHz, CDCl$_3$) δ 161.50 (d, J = 246.8 Hz), 157.63, 156.78, 155.95 (d, J = 7.3 Hz), 138.69, 129.36, 128.34 (2C), 127.95 (d, J = 10.2 Hz), 127.61 (2C), 127.46, 119.00, 117.51 (d, J = 18.2 Hz), 114.56, 114.46 (d, J = 3.3 Hz), 113.58, 110.52 (d, J = 22.3 Hz), 79.75, 78.84, 76.71, 72.86, 70.34, 29.28, 28.87 (3C), 28.70, 25.43, 18.74, 12.99 (d, J = 4.8 Hz).

4.1.21. 8-(2-(3-(*tert*-Butoxy)phenoxy)-6-fluorophenyl)octan-1-ol (17a)—

Treatment of **16a** as outlined in general procedure C provided **17a** as a yellow solid (95% yield). ^{1}H NMR (400 MHz, CDCl$_3$) δ 7.21 (t, J = 8.1 Hz, 1H), 7.09 (td, J = 8.2, 6.5 Hz, 1H), 6.83 (t, J = 8.8 Hz, 1H), 6.77 - 6.74 (m, 1H), 6.70 - 6.66 (m, 2H), 6.61 (t, J = 2.3 Hz, 1H), 3.62 (td, J = 6.6, 1.3 Hz, 2H), 2.67 (td, J = 7.6, 1.6 Hz, 2H), 1.61 - 1.51 (m, 4H), 1.36 (s, 9H), 1.33 - 1.26 (m, 8H). ^{13}C NMR (101 MHz, CDCl$_3$) δ 162.04 (d, J = 244.6 Hz), 158.02, 156.74, 155.84 (d, J = 8.3 Hz), 129.40, 126.85 (d, J = 10.4 Hz), 122.17 (d, J = 18.7 Hz), 118.68, 114.70 (d, J = 3.1 Hz), 114.02, 113.00, 110.50 (d, J = 23.1 Hz), 78.91, 63.00, 32.77, 29.43, 29.32, 29.25,

29.22, 28.84 (3C), 25.69, 22.98 (d, $J = 2.7$ Hz). ESI-MS m/z: 389.2 (MH$^+$), 333.1 (MH$^+$ - Bu).

4.1.22. 8-(2-(3-(Benzyloxy)phenoxy)-6-fluorophenyl)octan-1-ol (17b)—Treatment of **15b** with hept-6-yn-1-ol using CuI, Cs$_2$CO$_3$ and TBAI in acetonitrile (70 °C, 20 h) as the reported method[31] followed by using the synthesis as outlined in general procedure B provided **17b** as a colorless oil (9% yield). ^{1}H NMR (400 MHz, CDCl$_3$) δ 7.45 - 7.35 (m, 5H), 7.28 - 7.22 (m, 1H), 7.14 - 7.08 (m, 1H), 6.88 - 6.83 (m, 1H), 6.76 - 6.70 (m, 2H), 6.61 - 6.56 (m, 2H), 5.05 (s, 2H), 3.64 (t, $J = 6.6$ Hz, 2H), 2.67 (td, $J = 7.6$, 1.6 Hz, 2H), 1.62 - 1.52 (m, 4H), 1.33 (qt, $J = 8.3$, 3.2 Hz, 8H). ^{13}C NMR (101 MHz, CDCl$_3$) δ 162.06 (d, $J = 244.7$ Hz), 160.10, 158.87, 155.56 (d, $J = 8.3$ Hz), 136.68, 130.18, 128.61 (2C), 128.06, 127.56 (2C), 126.93 (d, $J = 10.3$ Hz), 122.42 (d, $J = 18.8$ Hz), 115.12 (d, $J = 3.1$ Hz), 110.71 (d, $J = 23.0$ Hz), 110.47, 109.29, 105.03, 70.15, 63.06, 32.78, 29.44, 29.35, 29.29 (2C), 29.26, 25.71, 23.06, 23.04. ESI-MS m/z: 423.2 (MH$^+$), 435.2 (MNa$^+$).

4.1.23. N^α-(((9H-Fluoren-9-yl)methoxy)carbonyl)-N^π-(8-(4-(2-(tertbutoxy) ethyl)phenyl)octyl)-L-histidine (18a)—Treatment of **11a** as outlined in general procedure G provided **18a** as a yellow oil (30% yield). DUIS-MS m/z: 667 (MH$^+$).

4.1.24. N^α-(((9H-Fluoren-9-yl)methoxy)carbonyl)-N^π-(8-(2-(3-(tertbutoxy) phenoxy)-6-fluorophenyl)octyl)-L-histidine (18b)—Treatment of **17a** as outlined in general procedure G provided **18b** as a yellow solid (30% yield). ESI-MS m/z: 748.3 (MH$^+$).

4.1.25. N^α-(((9H-Fluoren-9-yl)methoxy)carbonyl)-N^π-(8-(4-(2-(benzyloxy)ethyl)phenyl)octyl)-L-histidine (18c)—Treatment of **11b** as outlined in general procedure G provided **18c** as a colorless oil (64% yield). ESI-MS m/z: 700.3 (MH$^+$).

4.1.26. N^α-(((9H-Fluoren-9-yl)methoxy)carbonyl)-N^π-(8-(2-(3-(benzyloxy)phenoxy)-6-fluorophenyl)octyl)-L-histidine (18d)—Treatment of **11b** as outlined in general procedure G provided **18d** as a yellow oil (65% yield). ESI-MS m/z: 782.3 (MH$^+$).

4.1.27. General solid-phase peptide synthesis (SPPS—Protected amino acids used were Fmoc-Thr(PO(OBzl)OH)-OH, Fmoc-Ser(O^{t}Bu)-OH, $N(\pi)$-alkylated Fmoc-His-OH (**18a–d**), Fmoc-Leu-OH, and Fmoc-Pro-OH (purchased from Novabiochem). Peptides were synthesized on a NovaSyn® TGR resin (Novabiochem Cat#. 855009) using standard Fmoc solid-phase protocols in N-methyl-2-pyrrolidone (NMP). 1-[Bis(dimethylamino)methylene]-1H-1,2,3-triazolo[4,5-b]pyridinium 3-oxid hexafluorophosphate (HATU) (5.0 equivalents), and N,N-diisopropylethylamine (DIPEA) (10 equivalents) were used as coupling reagents. Unnatural amino acid residues were coupled using 2.5 equivalents. Deprotection was performed using 20% piperidine in DMF (15 min, twice). Amino-terminal acetylation was performed using 1-acetylimidazole. Finished resins were washed with NMP, MeOH, CH$_2$Cl$_2$, and Et$_2$O, dried under vacuum, and then cleaved by treatment with a solution of TFA:H$_2$O:TIS (95:2.5:2.5) (5 h). The resin was removed by filtration, and the filtrate was concentrated under vacuum and the resulting

residue dissolved in 50% aqueous acetonitrile (5 mL) and purified by reverse-phase preparative high pressure liquid chromatography (HPLC) using a Waters 2535 system having photodiode array detection and Phenomenex C18 columns (Cat. No. 00G-4436-P0-AX, 250 mm × 21.2 mm 10 μm particle size, 110 A pore) at a flow rate of 10 mL/min. Binary solvent systems consisting of A = 0.1% aqueous TFA and B = 0.1% TFA in acetonitrile were employed with gradients as indicated. Products (**6a, b** and **7a, b**) were obtained as amorphous solids following lyophilization.

4.1.28. Peptides

Peptide 6a: Title peptide **6a** was prepared using **18a** as outlined in SPPS and purified by preparative HPLC (linear gradient of 0% B to 80% B over 30 min, retention time = 17.7 min). ESI-MS *m/z*: 907.4 (MH$^+$). HRMS calcd for $C_{42}H_{68}N_8O_{12}P(MH^+)$ 907.4689, found 907.4676.

Peptide 6b: Title peptide **6b** was prepared using **18b** as outlined in SPPS and purified by preparative HPLC (linear gradient of 0% B to 80% B over 30 min, retention time = 19.7 min). ESI-MS *m/z*: 989.2 (MH$^+$). HRMS calcd for $C_{46}H_{67}FN_8O_{13}P(MH^+)$ 989.4544, found 989.4516.

Peptide 7a: Title peptide **7a** was prepared using **18c** as outlined in SPPS and purified by preparative HPLC (linear gradient of 0% B to 80% B over 30 min, retention time = 21.6 min). ESI-MS *m/z*: 997.3 (MH$^+$).

Peptide 7b: Title peptide **7b** was prepared using **18d** as outlined in SPPS and purified by preparative HPLC (linear gradient of 0% B to 80% B over 30 min, retention time = 22.3 min). ESI-MS *m/z*: 1079.2 (MH$^+$). HRMS calcd for $C_{53}H_{73}FN_8O_{13}P$ (MH$^+$) 1079.5013, found 1079.4993.

4.2 Biological Experimental Procedures

Experimental procedures used to obtain the IC$_{50}$ values shown in Table 1 have been previously reported[24] and are described in detail in the Supplementary data.

4.3. Comparison of the PBDs of Plk1, Plk2 and Plk3 in the region corresponding to the cryptic binding pocket of Plk1

4.3.1. ICM Modeling protocols—Standard Molsoft parameters and procedures were used as defined in the unmodified ICM Chemist Pro version 3.8-5/MacOSXIL64bit/g4.2/Release/HardwareGL/Gui264199/WebKit/Video/FlexLM built Oct 17 2016 14:22. 4.8.7.

4.3.2. Sequence alignment and identification of cryptic pocket residues—ICM Modeling was preformed using Plk1 (PDB accession code: 3RQ7), Plk2 (PDB accession code: 4RS6) and Plk3 [(Robetta homology model based on PDB accession code: 3FVH (see Supplementary data)]. Sequences were aligned using 3RQ7 as the static reference. The **2a** ligand from the 3RQ7 structure was placed in each structure based on the protein alignments, then all neighboring residues were minimized using the ICM standard protocol. Results are shown in Figure 3.

Supplementary Material

Refer to Web version on PubMed Central for supplementary material.

Acknowledgments

References and notes

1. Zitouni S, Nabais C, Jana SC, Guerrero A, Bettencourt-Dias M. Nat Rev Mol Cell Biol. 2014; 15:433–452. [PubMed: 24954208]

2. Lee KS, Burke TR, Park JE, Bang JK, Lee E. Trends Pharmacol Sci. 2015; 36:858–877. [PubMed: 26478211]

3. de Carcer G, Escobar B, Higuero AM, Garcia L, Anson A, Perez G, Mollejo M, Manning G, Melendez B, Abad-Rodriguez J, Malumbres M. Mol Cell Biol. 2011; 31:1225–1239. [PubMed: 21245385]

4. Elia AEH, Cantley LC, Yaffe MB. Science. 2003; 299:1228–1231. [PubMed: 12595692]

5. Strebhardt K. Nat Rev Drug Discov. 2010; 9:643–659. [PubMed: 20671765]

6. Park JE, Erikson RL, Lee KS. Proc Natl Acad Sci U S A. 2011; 108:8200–8205. [PubMed: 21525413]

7. Berg A, Berg T. ChemBioChem. 2016; 17:650–656. [PubMed: 26662918]

8. Reindl W, Strebhardt K, Berg T. Anal Biochem. 2008; 383:205–209. [PubMed: 18793607]

9. Reindl W, Graeber M, Strebhardt K, Berg T. Anal Biochem. 2009; 395:189–194. [PubMed: 19716361]

10. Archambault V, Lepine G, Kachaner D. Oncogene. 2015; 34:4799–4807. [PubMed: 25619835]

11. Yun SM, Moulaei T, Lim D, Bang JK, Park JE, Shenoy SR, Liu F, Kang YH, Liao C, Soung NK, Lee S, Yoon DY, Lim Y, Lee DH, Otaka A, Appella E, McMahon JB, Nicklaus MC, Burke TR Jr, Yaffe MB, Wlodawer A, Lee KS. Nat Struct Mol Biol. 2009; 16:876–882. [PubMed: 19597481]

12. Liu F, Park JE, Qian WJ, Lim D, Graber M, Berg T, Yaffe MB, Lee KS, Burke TR Jr. Nat Chem Biol. 2011; 7:595–601. [PubMed: 21765407]

13. Liu F, Park JE, Qian WJ, Lim D, Scharow A, Berg T, Yaffe MB, Lee KS, Burke TR. ACS Chem Biol. 2012; 7:805–810. [PubMed: 22292814]

14. Liu F, Park JE, Qian WJ, Lim D, Scharow A, Berg T, Yaffe MB, Lee KS, Burke TR. ChemBioChem. 2012; 13:1291–1296. [PubMed: 22570300]

15. Sledz P, Stubbs CJ, Lang S, Yang YQ, McKenzie GJ, Venkitaraman AR, Hyvoenen M, Abell C. Angew Chem, Int Ed. 2011; 50:4003–4006.

16. Tan YS, Sledz P, Lang S, Stubbs CJ, Spring DR, Abell C, Best RB. Angew Chem, Int Ed. 2012; 51:10078–10081.

17. Sledz P, Lang S, Stubbs CJ, Abell C. Angew Chem Int Ed Engl. 2012; 51:7680–7683. [PubMed: 22730171]

18. Liu F, Stephen AG, Waheed AA, Aman MJ, Freed EO, Fisher RJ, Burke TR Jr. ChemBioChem. 2008; 9:2000–2004. [PubMed: 18655064]

19. Zhao XZ, Hymel D, Burke TR Jr. Bioorg Med Chem Lett. 2016; 26:5009–5012. [PubMed: 27624074]

20. Qian W, Liu F, Burke TR Jr. J Org Chem. 2011; 76:8885–8890. [PubMed: 21950469]

21. Sonogashira K, Tohda Y, Hagihara N. Tetrahedron Lett. 1975; 16:4467–4470.

22. Fish PV, Ryckmans T, Stobie A, Wakenhut F. Bioorg Med Chem Lett. 2008; 18:1795–1798. [PubMed: 18313294]

23. Elia AE, Rellos P, Haire LF, Chao JW, Ivins FJ, Hoepker K, Mohammad D, Cantley LC, Smerdon SJ, Yaffe MB. Cell. 2003; 115:83–95. [PubMed: 14532005]

24. Hymel D, Burke TR Jr. ChemMedChem. 2017; 12:202–206. [PubMed: 27992122]

25. Shan HM, Wang T, Quan JM. Biochem Biophys Res Commun. 2015; 456:780–784. [PubMed: 25511705]

26. Kim JH, Ku B, Lee KS, Kim SJ. Proteins: Struct, Funct, Bioinf. 2015; 83:1201–1208.

27. Kim DE, Chivian D, Baker D. Nucleic Acids Res. 2004; 32:W526–W531. [PubMed: 15215442]

28. Qian WJ, Park JE, Lim D, Lai CC, Kelley JA, Park SY, Lee KW, Yaffe MB, Lee KS, Burke TR. Biopolymers Pept Sci. 2014; 102:444–455.

29. Jourdant A, Gonzalez-Zamora E, Zhu J. J Org Chem. 2002; 67:3163–3164. [PubMed: 11975589]

30. Bartoli G, Bosco M, Locatelli M, Marcantoni E, Melchiorre P, Sambri L. Org Lett. 2005; 7:427–430. [PubMed: 15673256]

31. Kwon Y, Cho H, Kim S. Org Lett. 2013; 15:920–923. [PubMed: 23373705]
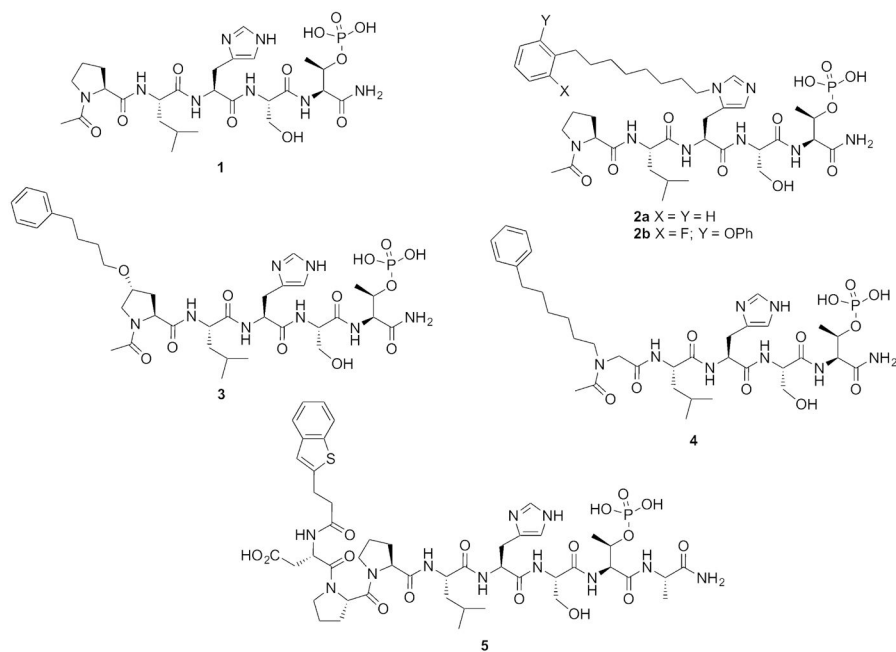
Figure 1.
Structures of peptides discussed in the text.
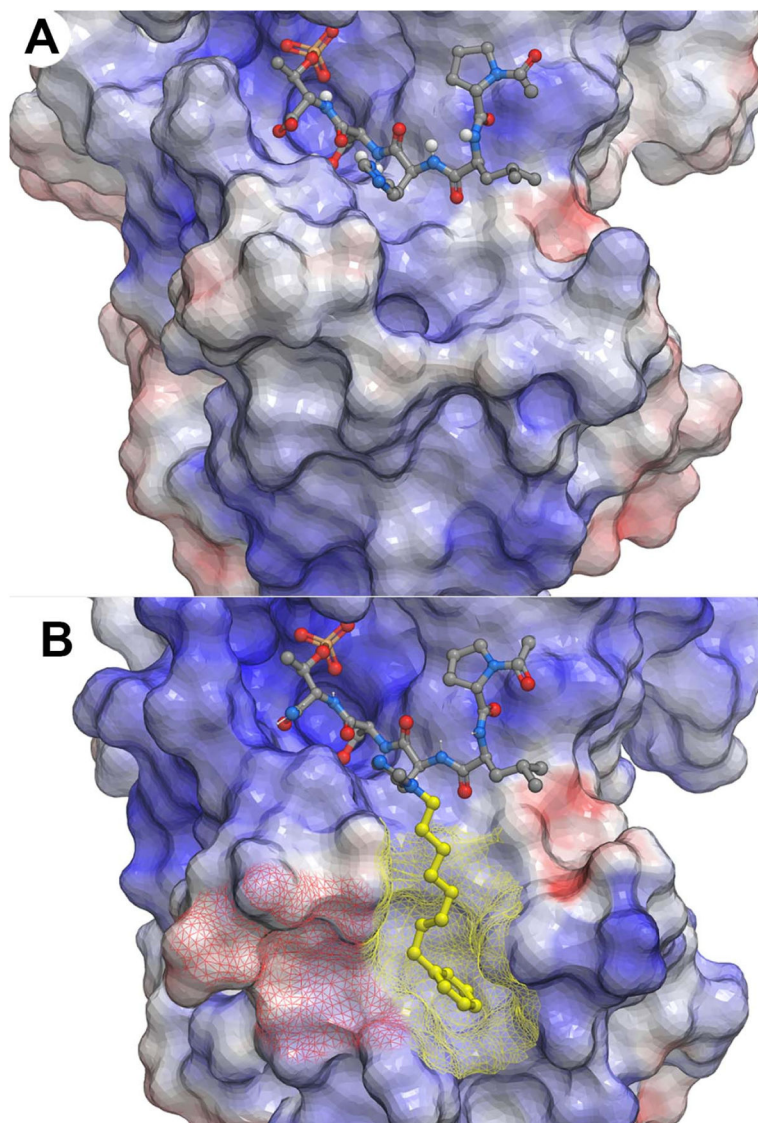
Figure 2.
Plk1 PBD electrostatic surfaces (blue = positive; red = negative). (A) PLHSpT with bound
1(PDB accession code: 3HIK); (B) PLH*SpT with bound **2a** (PDB accession code: 3RQ7)
having the portion of the peptide accessing the cryptic pocket shown in yellow and the
cryptic pocket overlain yellow mesh and a recently identified "auxiliary pocket" shown with
overlain red mesh.
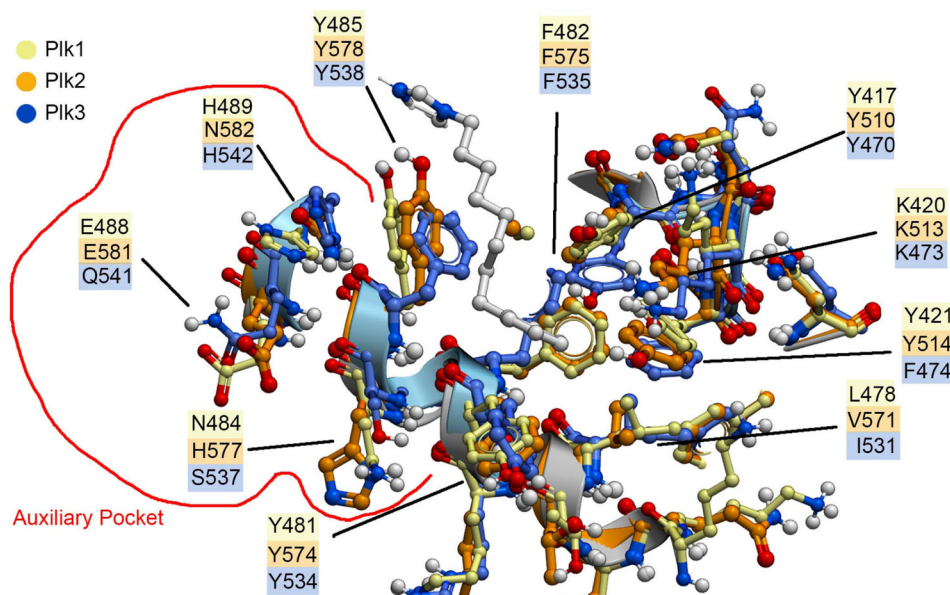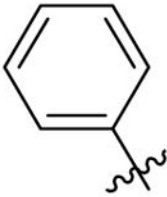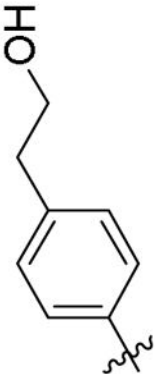
Figure 3.
Superposition of residues judged to potentially impact interactions in the cryptic pocket as well as in the "auxiliary pocket" (encircled in red). Residue carbons and residue numbering are color keyed as shown in the legend.
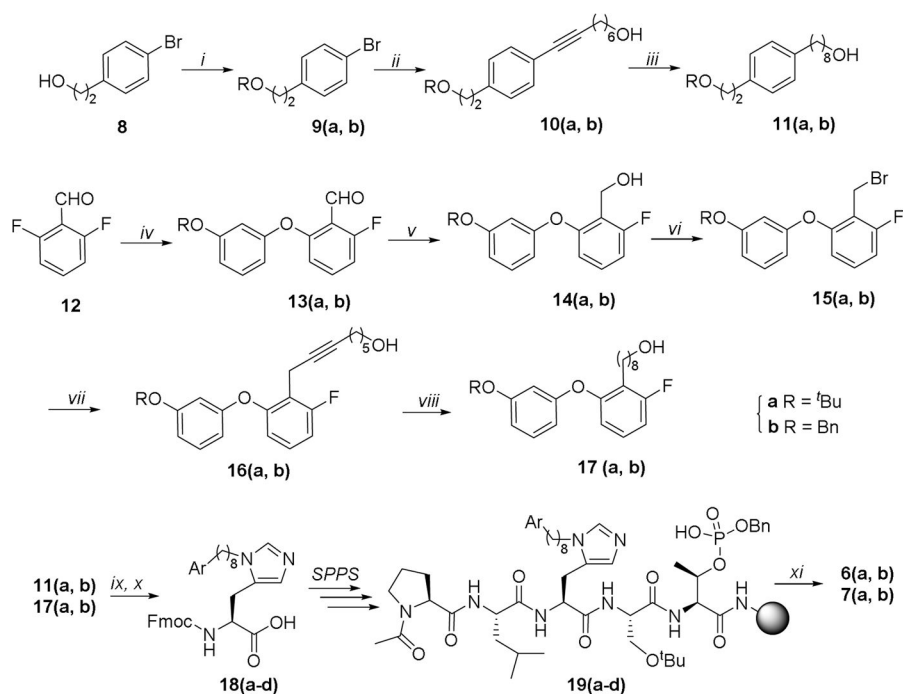
Scheme 1.

Preparation of peptides **6(a, b)** and **7(a, b)**. *Reagents and Conditions:* i) Boc$_2$O, Mg(ClO$_4$)$_2$; ii) Pd(PPh$_3$)$_2$Cl$_2$, CuI, CH≡C(CH$_2$)$_6$OH, 70 °C; iii) H$_2$, (Ph$_3$P)$_3$RhCl or Pd/C; iv) ArOH, K$_2$CO$_3$, DMA, 165 °C; v) NaBH$_4$, MeOH; vi) CBr$_4$, PPh$_3$, CH$_3$CN; vii) CuI, TBAI, Cs$_2$CO$_3$, CH≡C(CH$_2$)$_5$OH or ^{n}BuLi, CH≡C(CH$_2$)$_5$OBn; viii) CH≡CCH$_2$O^{t}Bu, CuI, DIEA, Pd(PPh$_3$)$_2$Cl$_2$; ix) N^α-Fmoc-His(N^τ-Trt)-OBn or N^α-Fmoc-His(N^τ-Trt)-ODMP, Tf$_2$O; x) TFA/TIS or H$_2$, Pd/C; xi) TFA/TIS/H$_2$O.

Table 1

Inhibitory binding potencies of peptides determined using full-length Plk1 and isolated PBDs of Plk1, Plk2 and Plk3.[i]

General Structures

No.	Ar	IC$_{50}$ (nM)[ii]				
		Plk1 ELISA	Plk1 PBD FP	Plk2 PBD FP	Plk3 PBD FP	
2a	(phenyl)	181 ± 13	5.0 ± 0.2	$130 \pm 10\ (26 \times)$ [iv]	$280 \pm 100\ (56 \times)$	
6a	(4-OH phenethyl)	218 ± 11	5.5 ± 0.2	$310 \pm 25\ (56 \times)$	$960 \pm 280\ (175 \times)$	
7a	(4-OBn phenethyl)	152 ± 4	9.7 ± 0.7	$250 \pm 20\ (25 \times)$	$920 \pm 100\ (95 \times)$	

General Structures

| No. | Ar | IC$_{50}$ (nM)[ii] | | | |
		Plk1 ELISA	Plk1 PBD FP	Plk2 PBD FP	Plk3 PBD FP
2b[iii]		127 ± 21	6.6 ± 0.3	290 ± 45 (44 ×)	$1,450 \pm 530$ (220 ×)

General Structures

No.	Ar	IC$_{50}$ (nM)[ii]			
		Plk1 ELISA	Plk1 PBD FP	Plk2 PBD FP	Plk3 PBD FP
6b		188 ± 22	5.5 ± 0.4	3,400 ± 60 (62 ×)	1,900 ± 540 (345 ×)

General Structures

No.	Ar	IC$_{50}$ (nM)[ii]			
		Plk1 ELISA	Plk1 PBD FP	Plk2 PBD FP	Plk3 PBD FP
7b		862 ± 113	11.2 ± 0.3	$3,500 \pm 800$ (312 ×)	$29,500 \pm 11,300$ (2,634 ×)

[i]Assays were conducted as described in the Experiment Section.

[ii]Values represent the average ± SEM from three independent experiments and fit using nonlinear regression in GraphPad Prism 6.

[iii]See reference.19

[iv]Selectivity compared with Plk1.